MiR-28-3p regulates high glucose-induced endothelial dysfunction by targeting CXXC5

Linjun Wang[1], Xin Fang[1], Yangmin Dong[2], Songmao Wang[2], Jun Pan[3], Ziheng Wu[3], Chenyang Qiu[3]*

[1]Department of Vascular Surgery, Affiliated Hangzhou First People's Hospital, Zhejiang University School of Medicine, Hangzhou, China
[2]Department of Vascular Surgery, Hangzhou Third People's Hospital, Hangzhou, China
[3]Department of Vascular Surgery, The First Affiliated Hospital, School of Medicine, Zhejiang University, Hangzhou, China

Submitted: 29 May 2023; **Accepted:** 14 August 2023
Online publication: 17 August 2023

Arch Med Sci
DOI: https://doi.org/10.5114/aoms/171024

***Corresponding author:**
Chenyang Qiu
Department of Vascular Surgery
The First Affiliated Hospital
School of Medicine
Zhejiang University
Hangzhou, China
E-mail: docqiu@zju.edu.cn

Abstract

Introduction: Data from the CEO database show that microRNA (miR)-28-3p levels are elevated in diabetic patients. Nevertheless, the role of miR-28-3p in peripheral artery disease with diabetes has not been investigated.
Material and methods: The levels of miR-28-3p, CXXC5, CXXC-type zinc finger protein 5, and CXXC5's downstream molecules as well as endothelial function were investigated. Dual luciferase analyses were used to confirm the binding site of miR-28-3p and CXXC5.
Results: Under high-glucose conditions, miR-28-3p expression is upregulated, whereas CXXC5 expression is downregulated. Overexpression of miR-28-3p increased cell apoptosis and inhibited cell proliferation, migration, and vessel formation, whilst inhibiting its expression had the opposite effect. The overexpression and inhibition of miR-28-3p could also influence both the mRNA and protein levels of CXXC5 and its known downstream molecules. Analysis of bioinformatics data revealed a potential binding site for miR-28-3p and CXXC5. Dual luciferase analyses demonstrated that miR-28-3p suppressed CXXC5 expression by targeting the 3′-untranslated region (3′-UTR) of CXXC5. Following that, we overexpressed both miR-28-3p and CXXC5. The level of CXXC5 and its known downstream signaling molecules decreased with miR-28-3p overexpression alone. As anticipated, co-overexpression of miR-28-3p and CXXC5 partially reversed the effect of miR-28-3p mimics.
Conclusions: These findings indicated that miR-28-3p regulated high glucose-induced endothelial dysfunction by targeting CXXC5.

Key words: miR-28-3p, high glucose, endothelial dysfunction, peripheral artery disease, CXXC5.

Introduction

As life expectancy increases, peripheral artery disease (PAD) is becoming an increasingly severe public health problem. PAD affects roughly 10% of the general population between the ages of 70 and 80 and can reach over 20% at age 80 [1, 2]. Clinical studies have shown that diabetes is one of the vital risk factors for PAD [3–5]. In PAD patients with critical limb ischemia, diabetes doubled all-cause mortality [5]. In addition, every 1% increase in HbA_{1c} would lead to a 14.2% increased relative risk for major adverse cardiovascular events [4]. The mecha-

nism by which diabetes worsens PAD prognosis remains unexplained.

MicroRNAs are a class of highly conserved, single-stranded, endogenous non-coding small molecule RNAs, 20–24 nucleotides in length. They are able to complementarily bind to the 3′ non-coding regions (3′UTRs) of their target mRNAs, inhibit the translation of mRNAs, and achieve post-transcriptional regulation, playing an indispensable role in cell development, proliferation, apoptosis and differentiation [6]. A few microRNAs, such as miR-21, miR-126, miR-143, and miR-221, have been demonstrated in the regulation of PAD, and provide a therapeutic approach for diagnosis and treatment of diabetes-related complications [7, 8]. miR-28-3p was found to be elevated in type 2 diabetes patients with a 10-year history [9]. In addition, miR-28-3p expression was significantly higher in type 2 diabetes patients with diabetic retinopathy than in type 2 diabetes patients without diabetic retinopathy [10], indicating that it was associated with the severity of diabetes. In this study, we found that miR-28-3p expression was elevated after analyzing Gene Expression Omnibus (GEO) data from newly diagnosed type 1 diabetes patients with uncontrolled blood glucose. Its effects on the vascular endothelial remain unknown. In our study, we investigated the function of miR-28-3p in human umbilical vein endothelial cells (HUVECs). Under high-glucose conditions, miR-28-3p expression is upregulated, whereas CXXC5 (CXXC-type zinc finger protein 5) expression is downregulated. Overexpression of miR-28-3p increased cell apoptosis and inhibited cell proliferation, migration, and vessel formation. We confirmed that miR-28-3p suppressed CXXC5 expression by targeting the 3′-untranslated region (3′-UTR) of CXXC5. CXXC5 functions as a transcriptional regulator by its direct interaction with DNA [11]. It plays a crucial role in the coordination of several signaling pathways, such as transforming growth factor β (TGF-β), Wnt/β-catenin, ATM/p53 [11], and MARK signaling. In addition, it regulates endothelial cell differentiation and vessel formation in the endothelium [12]. As anticipated, co-overexpression of CXXC5 and miR-28-3p partially reversed the endothelium dysfunction caused by miR-28-3p mimics.

Material and methods

GEO data bioinformatics analysis

Type 1 diabetes gene expression and microRNA expression of 12 samples and 10 control samples were downloaded from the GEO database (GEO accession: GSE55098, GSE55099,https://www.ncbi.nlm.nih.gov/geo/). We used Targetscan (https://www.targetscan.org/vert_80/), Starbase (https://starbase.sysu.edu.cn/), and miRDB (http://mirdb.org/) to analyze the microRNAs with potential bio-function.

Cell culture

We purchased HUVECs from the American Type Culture Collection cell bank. The cells were cultured in DMEM medium and maintained in a humidified atmosphere with 5% CO_2 at 37°C. To simulate high glucose effects, HUVECs were treated with 33 mM glucose for 24 or 48 h.

Reverse transcription-quantitative PCR (RT-qPCR)

We extracted total RNA from HUVECs using the Trizol Reagent (Aidlab Biotechnologies Co., Ltd) according to the manufacturer's protocol. Total RNA was then reverse transcribed into cDNA using Hiscript Reverse transcriptase (Nanjing Vazyme Biotech Co., Ltd.). We used U6 and GAPDH as the internal control for microRNA and proteins, respectively. The RT-qPCR reaction was conducted using the SYBR Green Master Mix (Nanjing Vazyme Biotech Co., Ltd.) at 50°C for 2 min, 95°C for 10 min, followed by 40 cycles of 95°C for 30 s, and 60°C for 30 s. We calculated the relative expression of each mRNA or miRNA using the 2-ΔΔCt method. The experiments were performed via QuantStudio6 (Applied Biosystems, Inc.). All the primers used are listed as follows: GAPDH Forward 5′- TCAAGAAGGTGGTGAAGCAGG -3′, Reverse 5′-TCAAAGGTGGAGGAGTGGGT -3′. CXXC5 Forward 5′- CCGCTCTCCCACTACTCTTC -3′, Reverse 5′- GAGGTAGGGTTGCTTTTGTCC -3′. Flk-1 Forward TACGTTGGAGCAATCCCTGT, Reverse TACACTTTCGCGATGCCAAG. TGF-β Forward CAGCAACAATTCCTGGCGATACCT, Reverse CGCTAAGGCGAAAGCCCTCAAT. U6 Forward 5′- CGCTTCGGCAGCACATATAC -3′, Reverse 5′- AAATATGGAACGCTTCACGA -3′. miR-28-3p F primer TGCGCCACTAGATTGTGAGCTC, loop primer GTCGTATCCAGTGCAGGGTCCGAGGTATTCGCACTGGATACGACTCCAGGAG. mircoRNA universal antisense primer, R primer: CCAGTGCAGGGTCCGAGGTATT.

Plasmid construction

To overexpress the CXXC5 gene, the FV144-ZsGreen-CON plasmid was used to construct CXXC5 overexpression vectors. The CXXC5 gene was obtained and amplified from the hCXXC5-OE plasmid. We used the Seamless Cloning technique to insert the CXXC5 gene into the FV144-ZsGreen-CON plasmid. All fragments generated through PCR amplification and recombinant plasmid were sequenced to validate mutations in each fragment.

Cell transfection

After seeding HUVECs into a 6-well plate at a density of $1x10^5$ cells per well, cells were cultured until they reached a confluence of 50–60%. Then, transfection of microRNAs and plasmids into HUVECs was performed using Lipofectamine 2000 (Invitrogen; Thermo Fisher Scientific, Inc.) following the manufacturer's protocol. Briefly, 5 µl of Lipofectamine 2000 was added to 200 µl of serum-free RPMI-1640 medium and incubated for 5 min at room temperature. Subsequently, an appropriate amount of miR-28-3p mimic, miR-28-3p inhibitor, negative control, or pcDNA was added to the Lipofectamine mixture and incubated for an additional 20 minutes at room temperature. The final transfection mixture was then added to each well and incubated with the cells at 37°C for 24 h. For the high glucose group, HUVECs were treated with 33 mM glucose for 24 or 48 h for the subsequent experiments.

Cell proliferation

HUVECs were firstly seeded into 96-well plates at 3×10^3 cells/well, and then cultured for 24 h and received transfection of microRNA or plasmid for 6 h. After removing the transfection buffer, the cells were incubated in a normal medium for another 24 h and received high glucose treatment for 48 h in the high glucose group. Following incubation, 10 µl of Cell Counting Kit-8 solution (CCK-8 kit, Elabscience Biotechnology Co., Ltd) was added to each well and incubated for another 4 h at 37°C. Finally, we measured the absorbance at a wavelength of 450 nm.

Cell migration

We used Transwell assays to detect the migration of HUVECs. HUVECs were suspended at a concentration of 4×10^5 cells/ml in serum-free RPMI1640 medium. 800 µl of 10% fetal bovine serum was added to each well on a 24-well plate. Then 200 µl of HUVECs were loaded in each Transwell plate (Corning, Inc.) and placed in the well. We used a cotton swab to remove cells that remained in the upper chamber after 24 h of incubation and fixed the cells that had migrated to the lower chamber with 70% iced ethanol for 1 h at room temperature. Then we stained cells in the lower chamber with 0.5% crystal violet for 20 min at room temperature. Using a light microscope, we observed migratory cells from each group and counted their numbers in three randomly chosen fields of view (magnification ×200; Olympus Corporation).

Apoptosis analysis by flow cytometry

We detected cell apoptosis using an AnnexinV-FITC/PI kit (Elabscience Biotechnology Co., Ltd) according to the manufacturer's instructions. Following transfection, cell collection, and preparation, the HUVECs were stained for 15 min in the dark at room temperature with 5 ml of Annexin V and 5 ml of PI. Using a BD FACSVerse flow cytometer (BD Biosciences Co., Ltd), apoptotic cells were studied, and we analyzed the data using FlowJo software Version 10.4. (FlowJo Co., Ltd).

Vessel formation assay

We dissolved the Matrigel (Corning) and kept the 24-well plates at 4°C overnight. Then, we added 100 µl of Matrigel to the 24-well plate, which was then centrifuged to remove bubbles. After centrifugation, the plates were incubated at 37°C for 1 h with 1×10^5 HUVECs added to each well. Following that, the cells were incubated for another 12 h and visualized by microscope. Vessel formation from each well was observed and counted in three randomly chosen fields of view (magnification ×100; Olympus Corporation) and analyzed by ImageJ software.

Protein extraction and Western blotting

We washed HUVECs at least twice with cold PBS buffer. Then, we added RIPA lysis buffer (Beyotime Institute of Biotechnology) supplemented with phenylmethanesulfonyl fluoride (Beyotime) and sodium orthovanadate (Beyotime) to each well, followed by a 30-minute incubation period on ice. Following lysis, cells were carefully scraped from one side of the cell plate and the resulting mixture of cell debris and the lysate was collected into a 1.5 ml centrifuge tube and centrifuged at 12,000 rpm for 5 min at 4°C. The supernatant was then collected and transferred to a 0.5 ml centrifuge tube. The total protein concentration was measured using the BCA method. Protein samples were subjected to SDS-PAGE (40 µg of proteins were loaded in each well) and then transferred to the PVDF membrane. Primary antibodies, including GAPDH (1 : 1000 Affinity), P65 (1 : 1000 Boster), p-p65 (1 : 1000 Affinity), TGF-B (1 : 1000 Abcam), P38 (1 : 1000 Bioss) and p-p38 (1 : 1000 Affinity), were incubated with the membrane overnight. Then we incubated the membranes with secondary antibodies (1 : 5000) at room temperature for another 2 h and used the enhanced chemiluminescence method to analyze the results.

Vector construction and dual-Luciferase activity assay

We used TargetScan (www.targetscan.org) to predict that CXXC5 (3′ UTR) was the binding site of miR-28-3p. We used a pYr-MirTarget miRNA target expression vector to contain a wild-type (WT) or mutant (Mut) CXXC5 untranslated region (3′UTR).

293T cells were seeded in 12-well plates (1×10^5 cells/well) to obtain a cell confluence of 50–60%. The microRNAs and plasmid were co-transfected into 293T cells via Lipofectamine 2000 (Invitrogen; Thermo Fisher Scientific, Inc.). After 48 h of incubation, luciferase activity was assessed through a dual luciferase reporter assay (Beyotime Biotechnology). We normalized firefly luciferase activity to Renilla luciferase activity.

Statistical analysis

We presented data as mean ± SD and used two-tailed Student's *t*-test to compare continuous data. Statistical analysis was performed via GraphPad Prism software version 5.0 (GraphPad Software, Inc.). *P*-values < 0.05 were considered statistically significant.

Results

miR-28-3p and CXXC5 expression in high-glucose conditions

Expression profiling including microRNAs and proteins was obtained from Gene Expression Omnibus (GSE55098, GSE 55099). A total of 12 newly diagnosed diabetes type 1 patients and 10 normal controls were collected and analyzed. Their demographic characteristics are shown in Supplementary Table SI. The two Gene Expression Omnibus datasets showed that the miR-28-3p level (Figure 1 A) was up-regulated and the CXXC5 level (Figure 1 B) was down-regulated (although not reaching statistical significance). To further confirm these results, we subjected HUVECs to high glucose conditions (33 mM glucose for 24 h and 48 h, respectively) to simulate diabetes. The results from HUVECs were consistent with GEO data, showing an increase in miR-28-3p level and decrease in CXXC5 level after exposure to high glucose (Figures 1 C, D).

miR-28-3p was related to high-glucose-induced endothelial dysfunction and regulated CXXC5 expression

We studied the effect of miR-28-3p on HUVECs. After transfection of HUVECs with miR-28-3p mimics as well as inhibitors, miR-28-3p level was significantly upregulated and downregulated, respectively (Figure 2 A). The effects of miR-28-3p

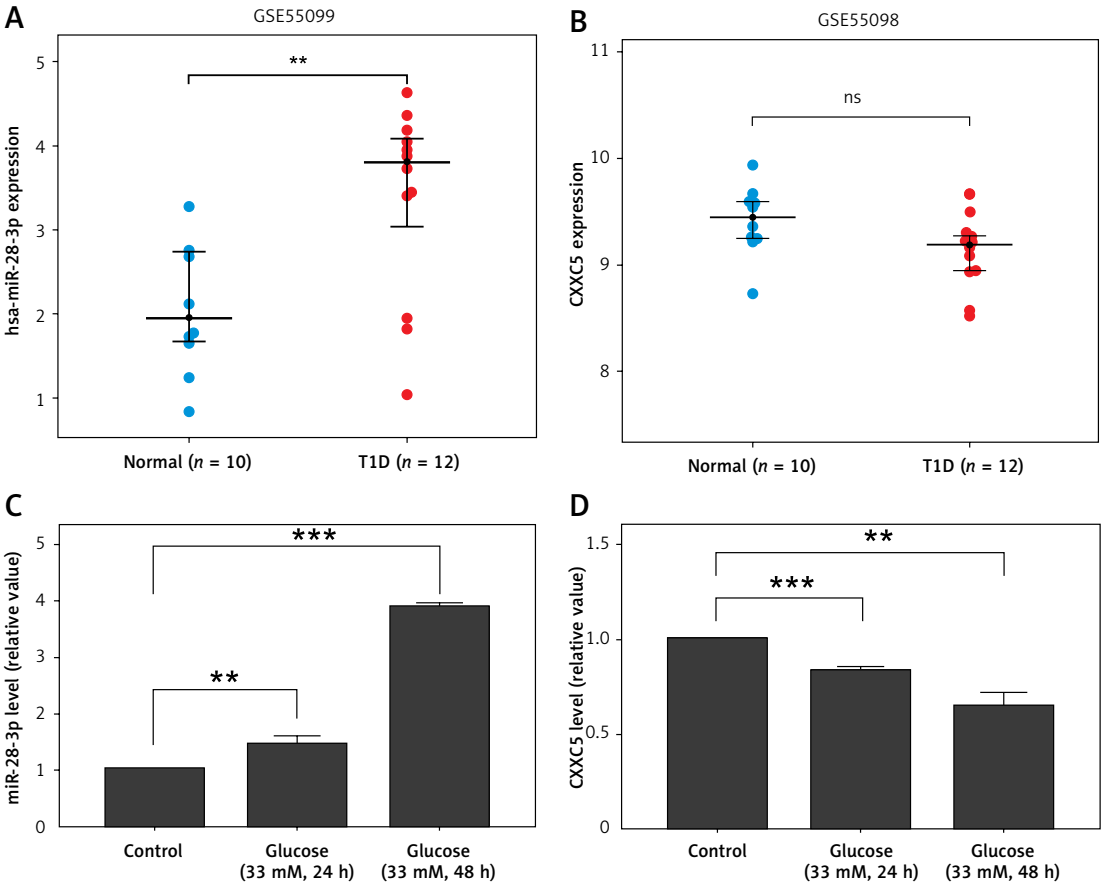

Figure 1. miR-28-3p and CXXC5 expression. the miR-28-3p level increased and the CXXC5 level decreased under high glucose conditions. The CXXC5 level in 1B showed a decrease among diabetic patients, though not reaching statistical significance. 12 diabetes patients vs 10 normal controls. **A**, **B** – from Gene Expression Omnibus (GSE55098, GSE 55099). **C**, **D** – HUVECs in normal glucose and high glucose. *p < 0.05, **p < 0.01, ***p < 0.001

on cell migration and death were then investigated via CCK8 and flow cytometry. CCK8 analysis revealed that transfection with miR-28-3p mimics under normal conditions could impair cell proliferation while transfection with miR-28-3p inhibitors under high glucose would reverse the cell proliferation (Figure 2 D). Flow cytometry showed that miR-28-3p mimics increased the apoptosis of HUVECs under normal condition while miR-28-3p inhibitors decreased the apoptosis under high glucose (Figure 2 C and Supplementary Figure S1). We also assessed the CXXC5 level and its known downstream signaling molecules, Flk-1 (a receptor for vascular endothelial growth factor, also named as vascular endothelial growth factor receptor 2) and TGF-β (transforming growth factor beta, a multifunctional cytokine regulating cell growth and differentiation). The PCR results showed that CXXC5 was decreased with miR-28-3p mimics and increased with miR-28-3p inhibitors (Figure 2 B), along with the synchronized expression of both Flk-1 (Figure 2 E) and TGF-β (Figure 2 F).

We also detected the role of miR-28-3p in migration and vessel formation. Transwell assays and ves-

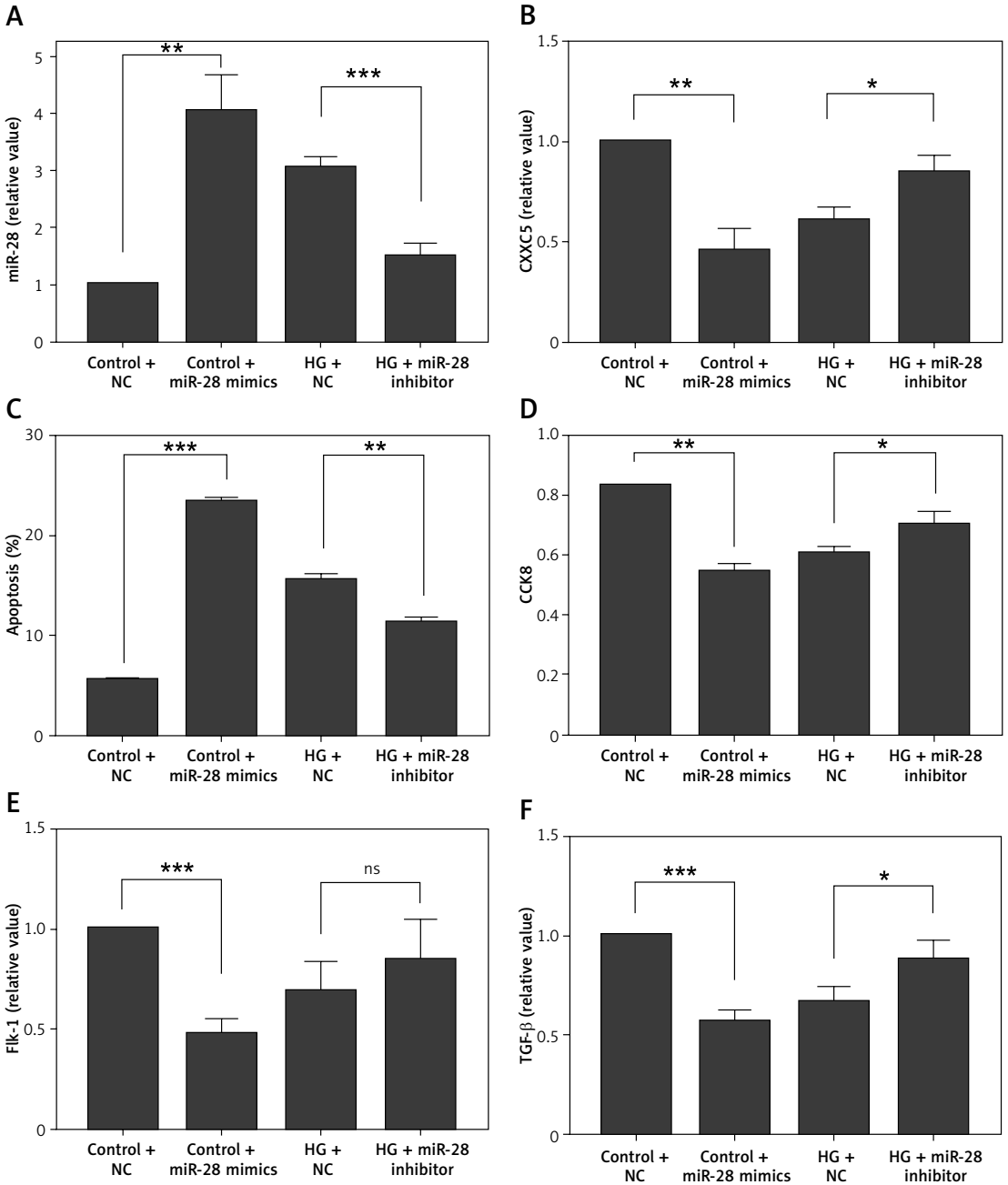

Figure 2. Molecular expression and HUVEC function under miR-28-3p mimics and inhibitors. **A**, **B**, **E**, **F** – PCR results; **C** – Apoptosis detected by flow cytometry. **D** – Cell proliferation assessed by CCK8. *$P < 0.05$, **$p < 0.01$, ***$p < 0.001$

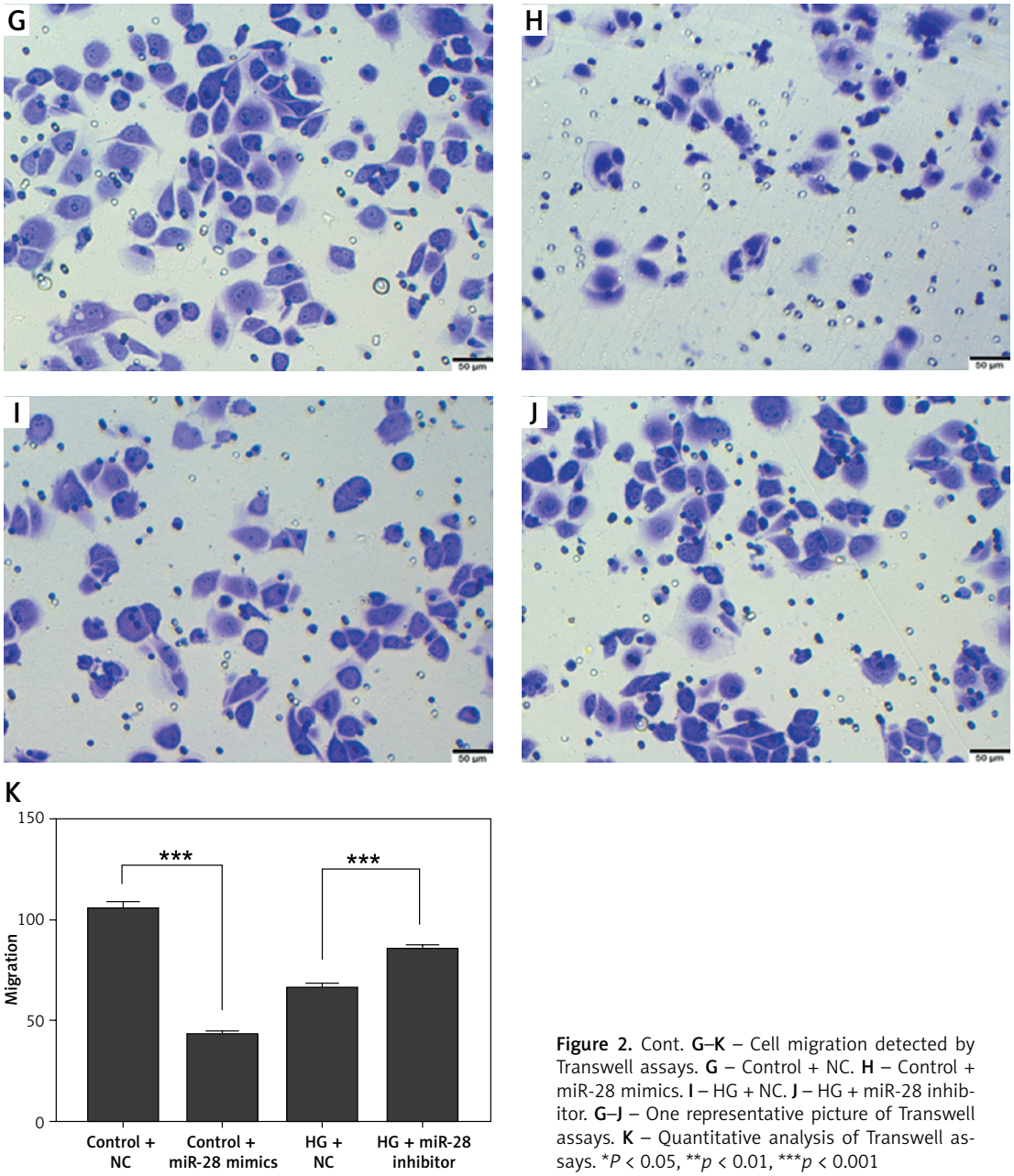

Figure 2. Cont. **G–K** – Cell migration detected by Transwell assays. **G** – Control + NC. **H** – Control + miR-28 mimics. **I** – HG + NC. **J** – HG + miR-28 inhibitor. **G–J** – One representative picture of Transwell assays. **K** – Quantitative analysis of Transwell assays. *$P < 0.05$, **$p < 0.01$, ***$p < 0.001$

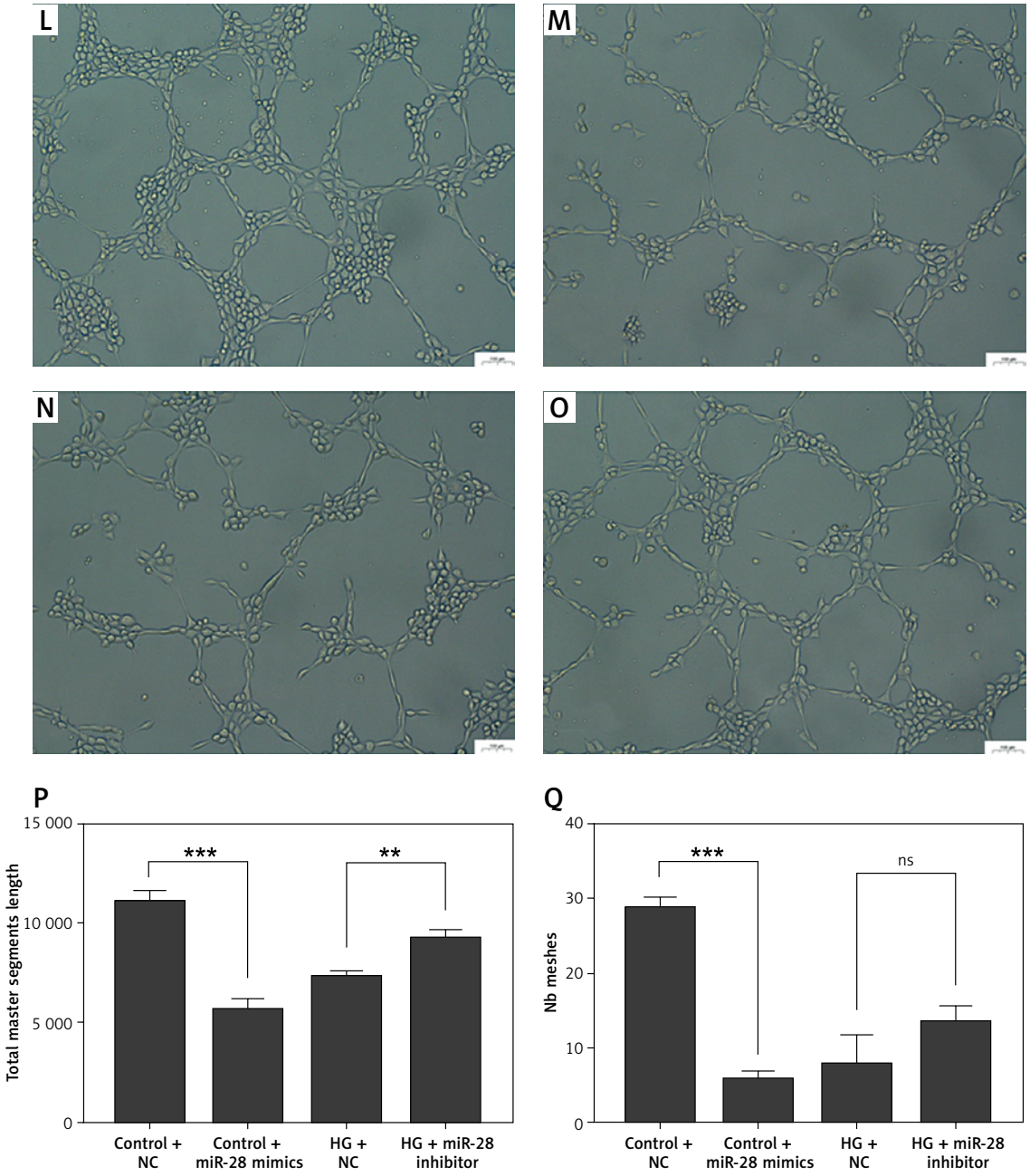

Figure 2. Cont. **L**–**Q** – Vessel formation assay. **L** – Control + NC. **M** – Control + miR-28 mimics. **N** – HG + NC. **O** – HG + miR-28 inhibitor. **L**–**O** – One representative picture of vessel formation assay. **P**, **Q** – Quantitative analysis of vessel formation. *$P < 0.05$, **$p < 0.01$, ***$p < 0.001$

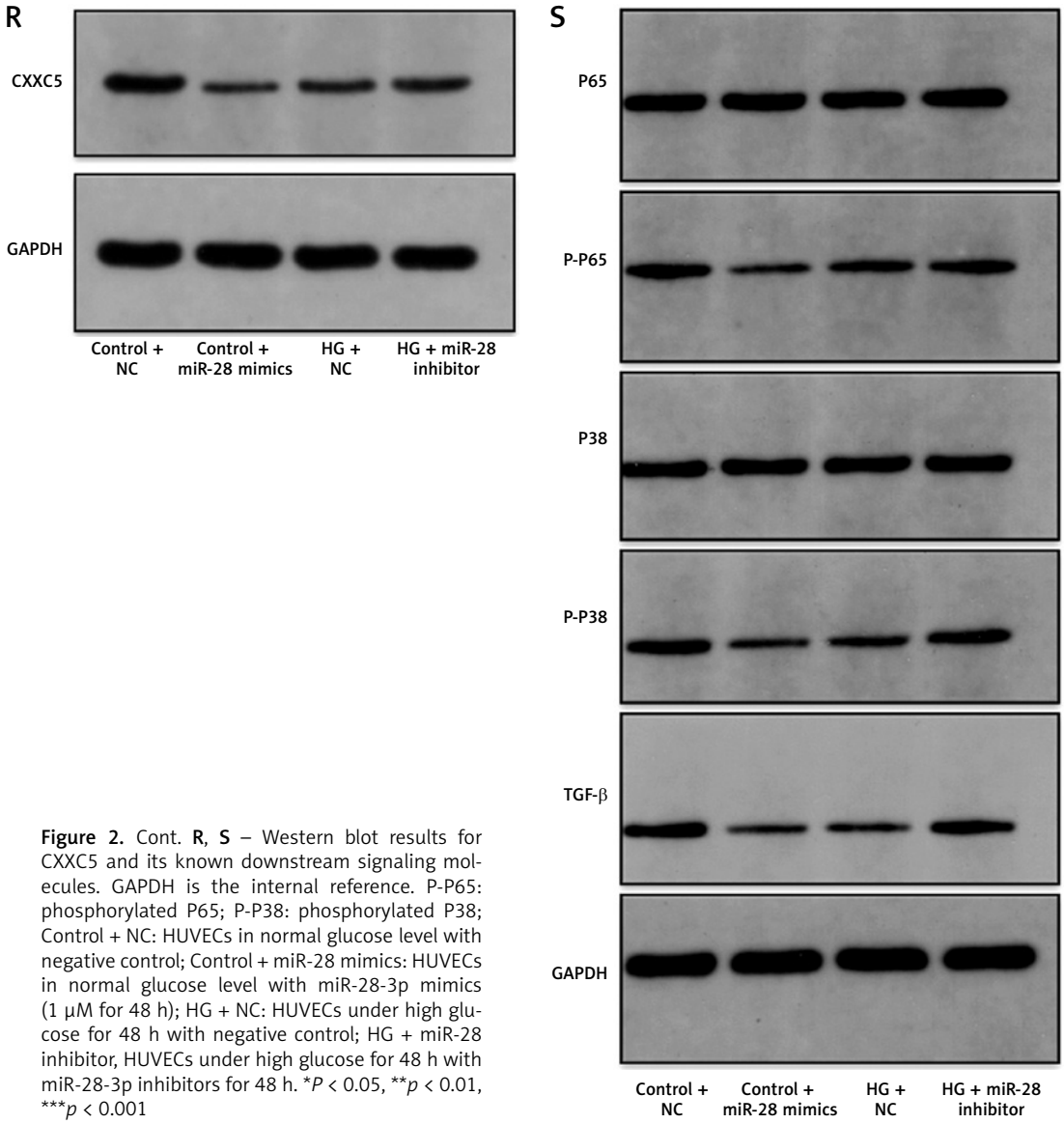

Figure 2. Cont. **R**, **S** – Western blot results for CXXC5 and its known downstream signaling molecules. GAPDH is the internal reference. P-P65: phosphorylated P65; P-P38: phosphorylated P38; Control + NC: HUVECs in normal glucose level with negative control; Control + miR-28 mimics: HUVECs in normal glucose level with miR-28-3p mimics (1 μM for 48 h); HG + NC: HUVECs under high glucose for 48 h with negative control; HG + miR-28 inhibitor, HUVECs under high glucose for 48 h with miR-28-3p inhibitors for 48 h. *$P < 0.05$, **$p < 0.01$, ***$p < 0.001$

sel formation assays showed that HUVECs' abilities of migration and vessel formation were significantly lower under miR-28-3p overexpression compared with those in the NC group (Figures 2 G, H, L M). On the other hand, the migration and vessel formation were significantly higher in the miR-28-3p inhibitor group compared with those in the inhibitor NC group (Figures 2 I, J, N, O). Figures 2 K, P and Q showed quantitative results of migration and vessel formation, respectively. These results suggested that miR-28-3p played a negative role in high glucose-induced endothelial dysfunction. In addition, we detected the effects of miR-28-3p on CXXC5 and its known downstream signaling molecules, TGF-β, P38, and P65, through Western blot. Similar expression patterns for CXXC5 were revealed by Western blot and PCR (Figure 2 R). CXXC5's known downstream signaling molecules exhibited synchronized expression patterns (Figure 2 S).

CXXC5 serves as a direct target gene of miR-28-3p

We used miRDB (http://mirdb.org/), Targetscan (https://www.targetscan.org/vert_80/), and Starbase (https://starbase.sysu.edu.cn/) to predict the possible gene target of miR-28-3p. The 3′-UTR of CXXC5 was predicted to have a complementary binding site for the seed region of miR-28-3p (Figures 3 A, B). To further test whether miR-28-3p targeted CXXC5, we used a dual luciferase reporter assay to determine their relationship in the 293T cell line. As shown in Figure 3 C, transfection with the miR-28-3p mimic led to a significant reduction in terms of the luciferase activity of the CXXC5-WT 3′-UTR compared with those transfected with mimic NC. The effect disappeared when the binding site of the CXXC5 3′-UTR was mutated, which suggested that CXXC5 may be a direct target gene of miR-28-3p.

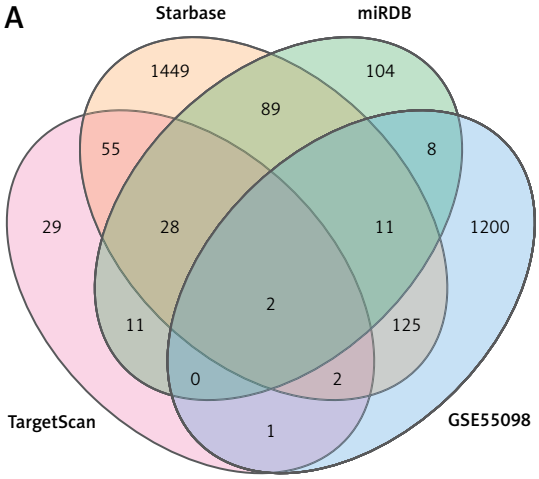

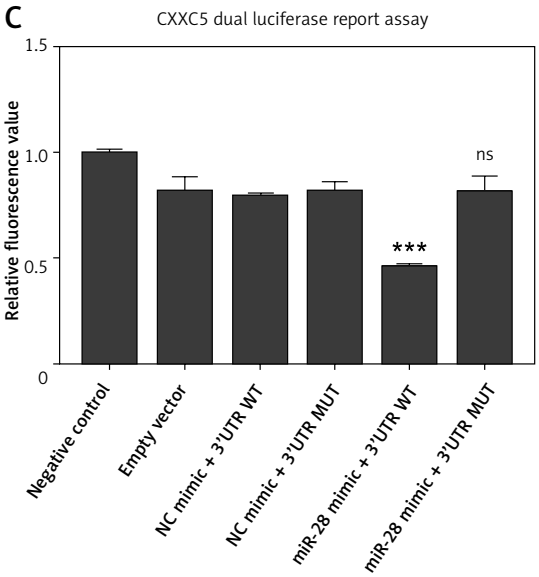

Figure 3. CXXC5 is a direct target gene of miR-28-3p. **A** – We used Targetscan, Starbase, and miRDB to predict the possible gene target of miR-28-3p in GSE55098, a dataset consisting of proteins from newly diagnosed type 1 diabetic patients. Only two proteins, namely CXXC5 and PARP8, poly(ADP-ribose) polymerase family member 8, were found to be the potential target. No correlation was observed between the expression levels of PARP8 and miR-28-3p in high-glucose cultured HUVEC. Therefore, the subsequent investigations were centered on miR-28-3p and CXXC5. **B** – Prediction of miR-28-3p binding sites in the 3′-UTR of the CXXC5 gene, along with the mutated 3′ UTR for dual luciferase reporter assay. **C** – Dual luciferase reporter assay. Transfection with the miR-28-3p mimic significantly decreased the relative luciferase activity of the CXXC5-WT 3′-UTR compared with that in cells following the transfection of mimic NC. The effect was abolished when the nucleotides in the seed binding site of the CXXC5 3′-UTR were mutated. $^{*}P < 0.05$, $^{**}p < 0.01$, $^{***}p < 0.001$

Effect of miR-28-3p mimics and CXXC5 overexpression in HUVECs

To further understand the mechanism of miR-28-3p and CXXC5 affecting HUVEC function, the effects of their overexpression on HUVEC function and CXXC5 downstream molecules were investigated. As illustrated in Figure 4, these results indicated that transfection with the miR-28-3p mimics significantly increased apoptosis (also refer to Supplementary Figure S2) and reduced cell proliferation. The level of CXXC5 and its downstream molecules, Flk-1 and TGF-β, were decreased. Intriguingly, the co-overexpression of CXXC5 partially reversed the effects of the miR-28-3p mimic on endothelial dysfunction and its downstream molecules.

We also evaluated the effect of co-overexpression of both miR-28-3p and CXXC5 on migration and vessel formation. Transwell assays (Figures 4 G–J) and vessel formation assays (Figures 4 K–O) revealed that the migratory and vessel formation abilities of HUVECs were significantly reduced in the miR-28-3p mimic group, and the effects were partially reversed when CXXC5 was overexpressed at the same time. In addition, we detected the effects of co-overexpression of both miR-28-3p and CXXC5 and its known downstream signaling molecules, TGF-β, P38, and P65, through Western blot. As anticipated, the level of CXXC5 and its downstream signaling molecules, TGF-β, phosphorylated P38, and phosphorylated P65, was decreased with miR-28-3p mimics, and the overexpression of CXXC5 partially reversed the effect of miR-28-3p mimics (Figures 4 P, R).

Discussion

PAD is characterized by narrowed arteries reducing blood flow to the lower extremities and becomes complicated when the patients have comorbidities such as diabetes and hypertension [4, 13].

Several microRNAs, including miR-142, miR-221, miR-143, miR-21, and miR-210, have been identified in the natural progression of PAD [14–16]. Targeting the microRNAs in exosomes may be a viable therapeutic technique for the treatment of cardiovascular complications associated with diabetes [7]. In addition, there are trials using locked nucleic acid-modified microRNA to inhibit the corresponding microRNA that was overexpressed in disease states [17]. miR-28-3p has been demonstrated to have a biological function in several diseases. The level of circulating miR-28-3p is significantly altered in several diseases, including severe asthma [18], colorectal cancer [19], gastric cancer [20], amyotrophic lateral sclerosis [21], non-ST-segment elevation acute coronary syndrome [22], pulmonary embolism [23], prostate cancer [24], diabetes with coronary heart disease [25], and diabetic retinopathy [10], and can be a marker for detecting these diseases. Previous studies have also shown that miR-28-3p inhibited prostate cancer cell proliferation and migration as well as

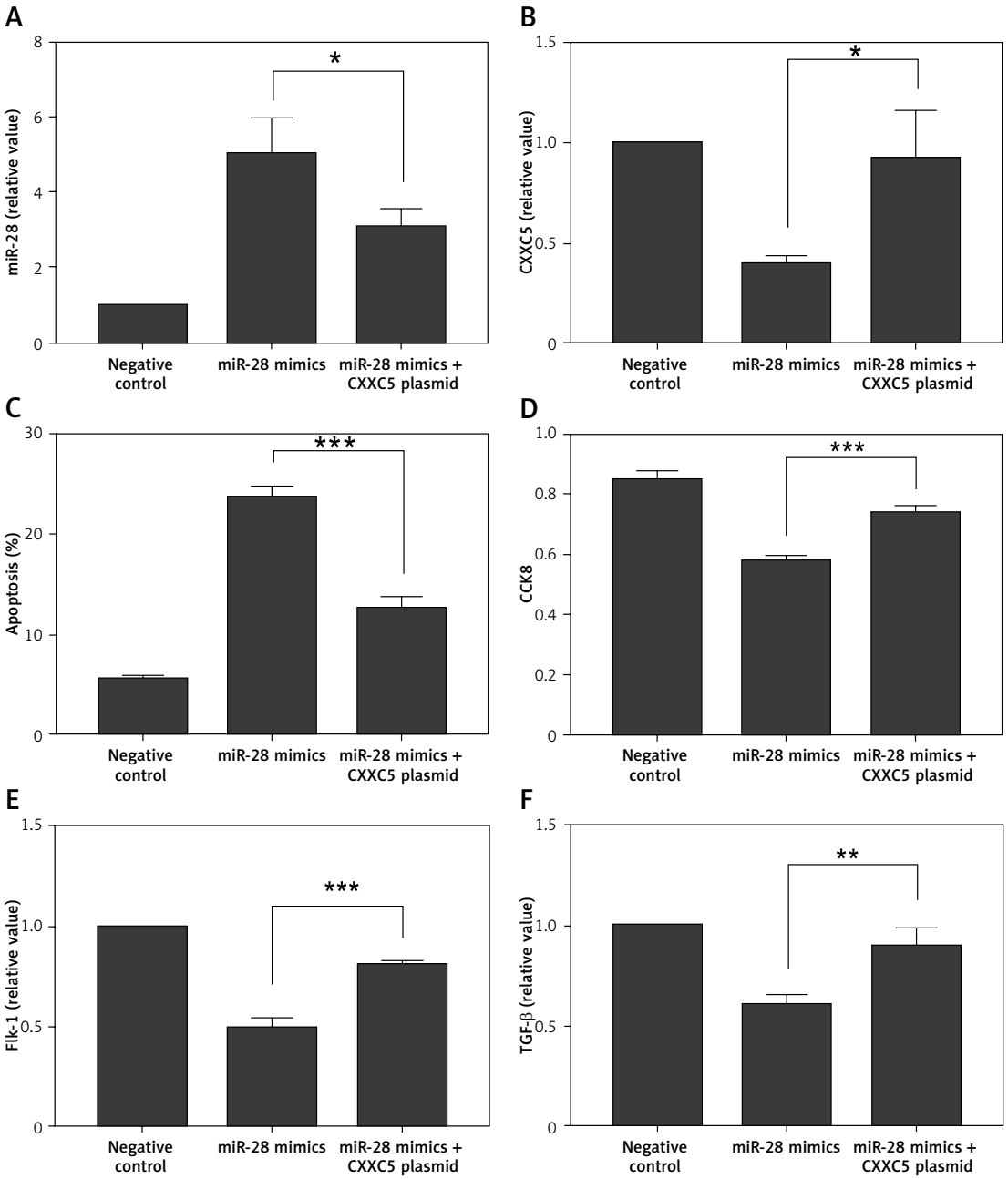

Figure 4. Molecular expression and HUVEC function under miR-28-3p mimics and CXXC5 overexpression. **A**, **B**, **E**, **F** – PCR results; **C** – Apoptosis detected by flow cytometry. D – Cell proliferation assessed by CCK8. **A**, **B**, **E**, **F** – PCR results. **C** – Apoptosis detected by flow cytometry; **D** – Cell proliferation assessed by CCK8. **P* < 0.05, ***p* < 0.01, ****p* < 0.001

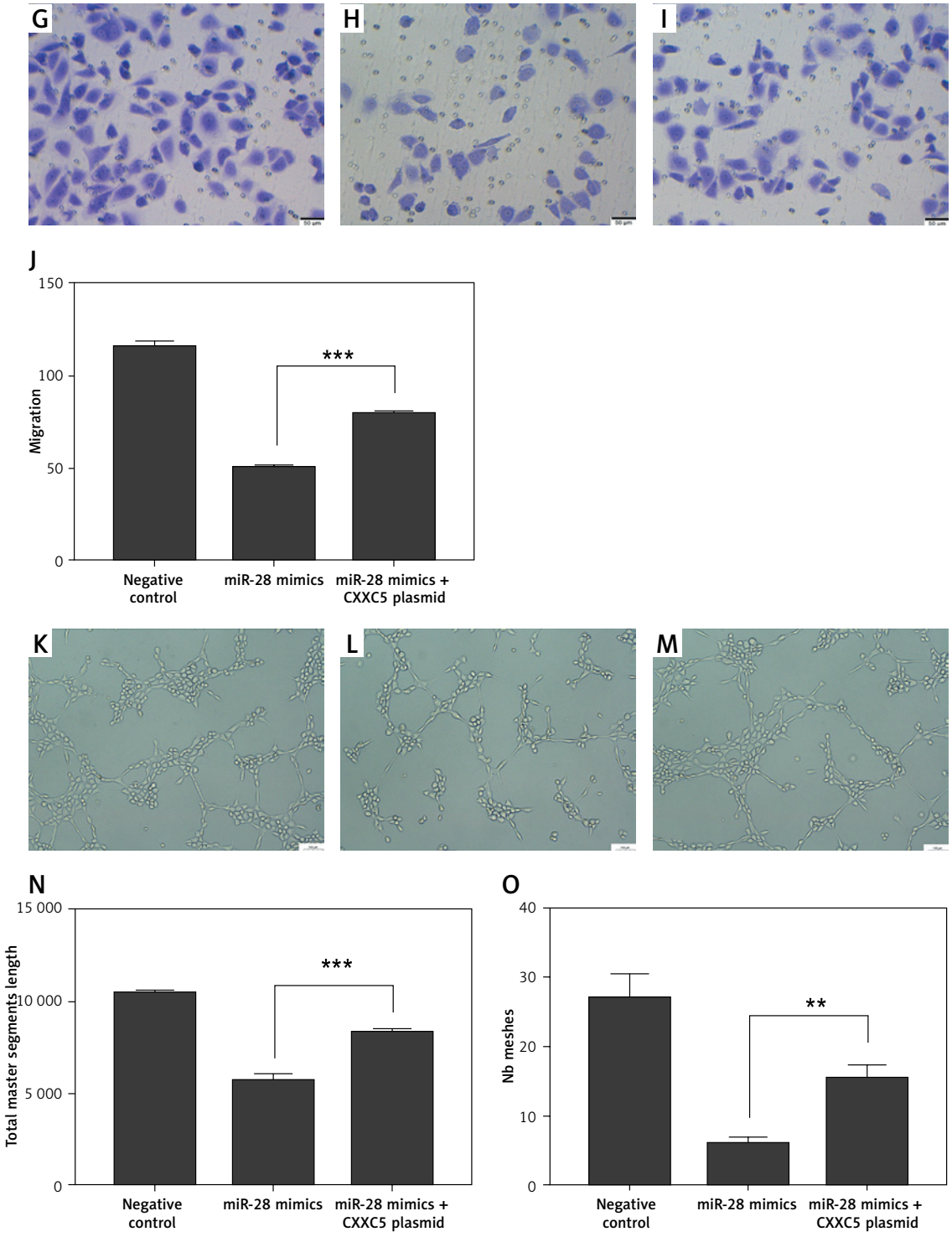

Figure 4. Cont. **G–J** – Cell migration detected by Transwell assays. Cell migration detected by Transwell assays. **G** – Negative control. **H** – miR-28 mimics. **I** – miR-28 mimics + CXXC5 plasmid. **G–I** – One representative picture of vessel formation assay. **J** – Quantitative analysis of Transwell assays. **K–O** – Vessel formation assay. **K** – Negative control. **L** – miR-28 mimics. **M** – miR-28 mimics + CXXC5 plasmid. **K–M** – One representative picture of vessel formation assay. **N**, **O** – Quantitative analysis of vessel formation. *$P < 0.05$, **$p < 0.01$, ***$p < 0.001$

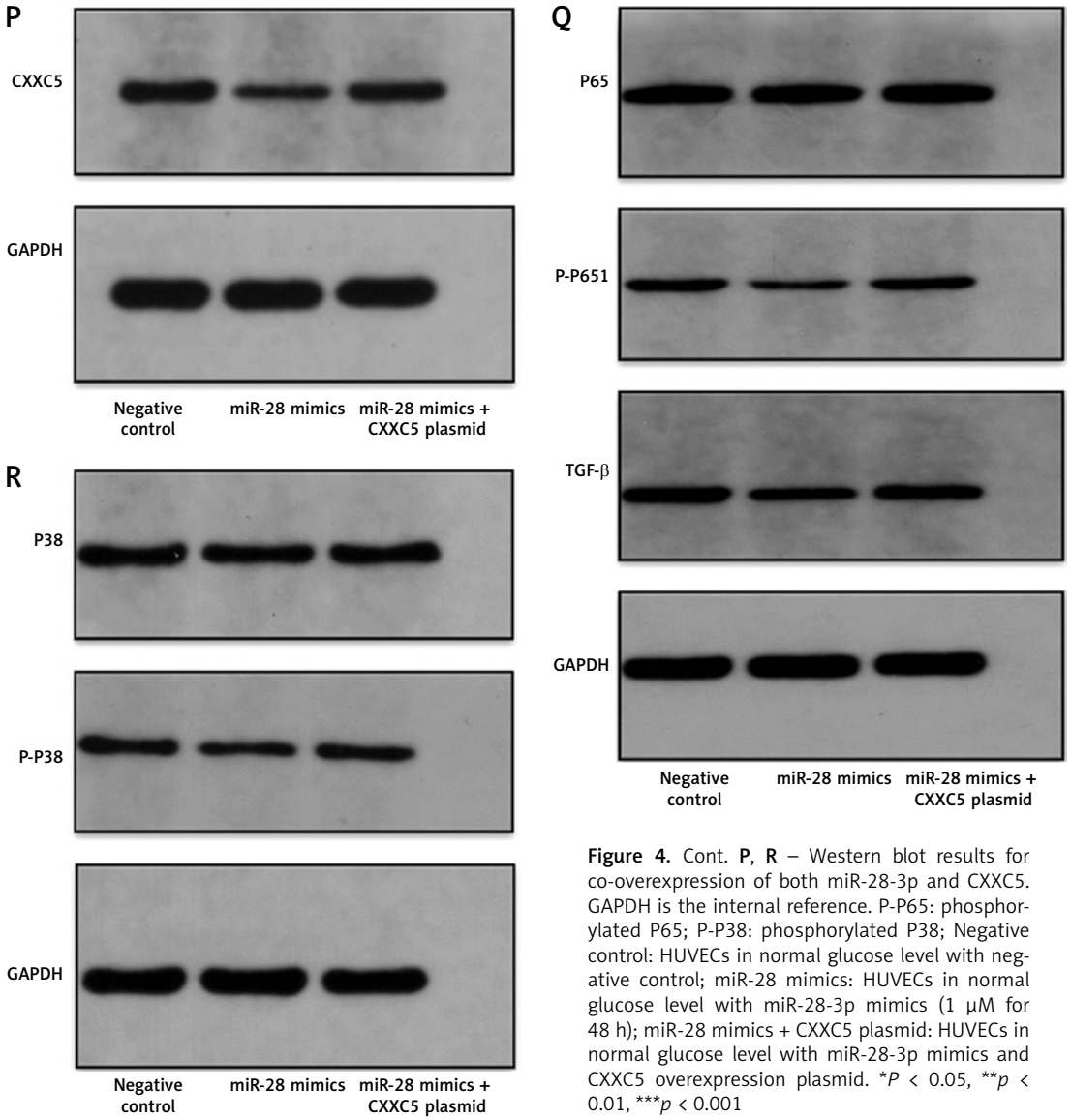

Figure 4. Cont. **P**, **R** – Western blot results for co-overexpression of both miR-28-3p and CXXC5. GAPDH is the internal reference. P-P65: phosphorylated P65; P-P38: phosphorylated P38; Negative control: HUVECs in normal glucose level with negative control; miR-28 mimics: HUVECs in normal glucose level with miR-28-3p mimics (1 μM for 48 h); miR-28 mimics + CXXC5 plasmid: HUVECs in normal glucose level with miR-28-3p mimics and CXXC5 overexpression plasmid. *$P < 0.05$, **$p < 0.01$, ***$p < 0.001$

invasion, promoted apoptosis by targeting ARF6 [26], and regulated myogenic differentiation and inhibition of rhabdomyosarcoma progression [27]. It also played a role in cell migration and invasion in nasopharyngeal cancer cells [28] and non-small cell lung cancer cells [29]. Nevertheless, there have been no previous reports on the role of miR-28-3p in PAD with diabetes.

In the present study, we used data from the GEO database to analyze the microRNAs with potential bio-function. The expression of miR-28-3p was found to be upregulated while CXXC5 was downregulated in diabetic patients compared with healthy controls in both GEO databases and further verified in HUVECs. Therefore, we hypothesized that miR-28-3p might play a role in endothelial function with high glucose. To confirm this hypothesis, we used HUVECs with high glucose to simulate PAD with diabetes. We discovered that miR-28-3p overexpression would induce cell apoptosis and inhibit cell proliferation and migration as well as vessel formation, while the inhibition of its expression showed the opposite effect. The overexpression and inhibition of miR-28-3p could also regulate the CXXC5 level and its known downstream molecules at both the mRNA and protein level. In addition, bioinformatics analysis showed a possible binding site for miR-28-3p and CXXC5. These data indicated that CXXC5 may be involved in miR-28-3p-mediated HUVEC function.

As one member of the CXXC-type zinc-finger protein family, CXXC5 is able to act as a transcriptional regulator by directly binding to DNA [11]. CXXC5 gene expression is regulated by a number of cytokines, intracellular transcription factors, and microRNAs [30]. In addition, CXXC5 itself plays an important role in coordinating various signaling pathways, including those initiated by TGF-β, bone and morphogenetic proteins, Wnt/β-catenin, ATM/p53 [11], and MARK signaling (Erk 1/2, p38,

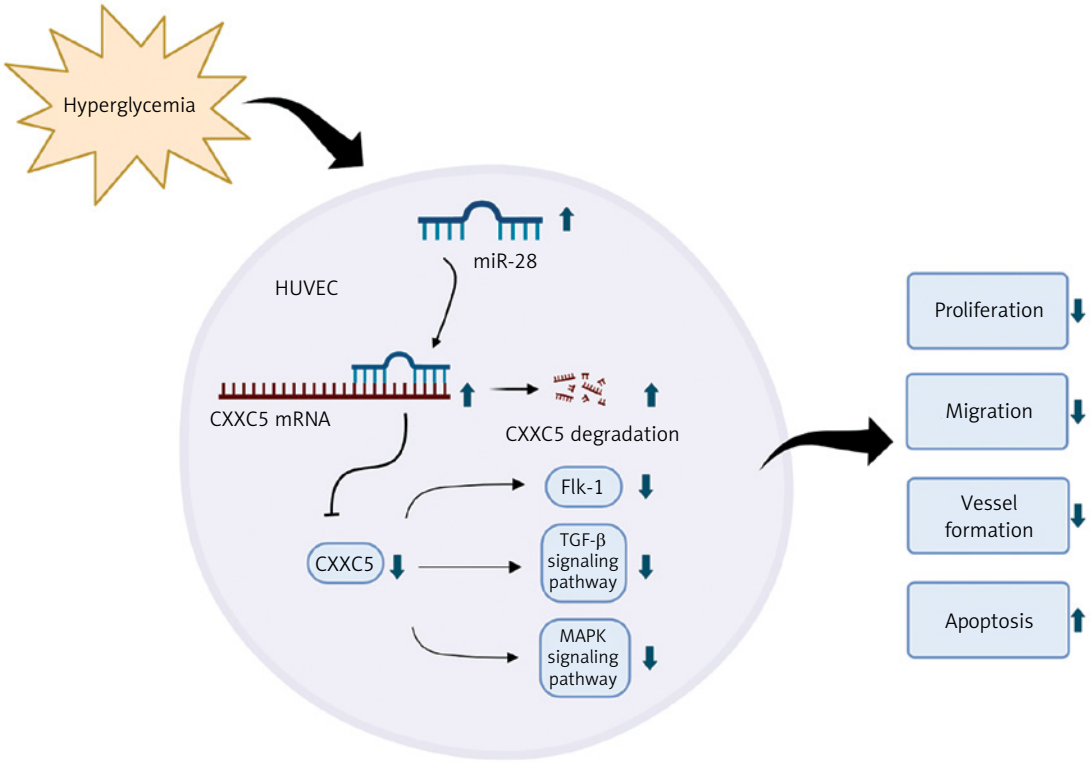

Figure 5. Diagram of the role of miR-28 in high glucose-cultured HUVEC

and c-Jun N-terminal kinase) [31]. CXXC5 is related to cell apoptosis in hepatocellular carcinoma [32], esophageal squamous cell carcinoma [30], and gastric cancer [33], and downregulation of CXXC5 is associated with a better prognosis in acute myeloid leukemia [34]. Additionally, CXXC5 is able to negatively regulate cutaneous wound healing [35]. In terms of endothelial function, it is reported to be a transcriptional activator of Flk-1, regulating endothelial cell differentiation and vessel formation [12].

In the current study, the luciferase assay indicated that miR-28-3p inhibited the expression levels of CXXC5 by targeting the 3′-UTR of CXXC5. Also, we overexpressed both miR-28-3p and CXXC5. As expected, the level of CXXC5 and its known downstream signaling molecules was decreased with miR-28-3p mimics alone, while the overexpression of CXXC5 at the same time partially reversed the effect of miR-28-3p mimics.

In conclusion, our study provided experimental *in vitro* evidence indicating that miR-28-3p inhibits vascular endothelial function by targeting CXXC5 in high-glucose cultured HUVECs. The limitation is the lack of *in vivo* experiments. There is still a long way ahead to translate the basic medical research of miR-28-3p into clinical application. The mechanisms revealed by our results imply that miR-28-3p may serve as a promising target in the treatment of PAD with diabetes (Figure 5).

Funding

This study was supported by the Health Commission of Zhejiang Province (Grant No. 2021KY904) and the National Natural Science Foundation of China (Grant No. 81970694).

Ethical approval

The authors are accountable for all aspects of the work in ensuring that questions related to the accuracy or integrity of any part of the work are appropriately investigated and resolved. Experiments were performed under a project license granted by the Institutional Review Board of the Ethics Committee of Zhejiang University, in compliance with Chinese guidelines for the care and use of animals.

Conflict of interest

The authors declare no conflict of interest.

References

1. Fowkes FG, Aboyans V, Fowkes FJ, et al. Peripheral artery disease: epidemiology and global perspectives. Nat Rev Cardiol 2017; 14: 156-70.
2. Song P, Rudan D, Zhu Y, et al. Global, regional, and national prevalence and risk factors for peripheral artery disease in 2015: an updated systematic review and analysis. Lancet Glob Health 2019; 7: e1020-30.
3. Cai M, Xie Y, Bowe B, et al. Temporal trends in incidence rates of lower extremity amputation and associated risk

factors among patients using Veterans Health Administration Services from 2008 to 2018. JAMA Netw Open 2021; 4: e2033953.
4. Low Wang CC, Blomster JI, Heizer G, et al. Cardiovascular and limb outcomes in patients with diabetes and peripheral artery disease: the EUCLID trial. J Am Coll Cardiol 2018; 72: 3274-84.
5. Vrsalovic M, Vucur K, Vrsalovic Presecki A, et al. Impact of diabetes on mortality in peripheral artery disease: a meta-analysis. Clin Cardiol 2017; 40: 287-91.
6. Van Meter EN, Onyango JA, Teske KA. A review of currently identified small molecule modulators of microRNA function. Eur J Med Chem 2020; 188: 112008.
7. Zhao S, Wang H, Xu H, et al. Targeting the microRNAs in exosome: a potential therapeutic strategy for alleviation of diabetes-related cardiovascular complication. Pharmacol Res 2021; 173: 105868.
8. Kumar S, Williams D, Sur S, et al. Role of flow-sensitive microRNAs and long noncoding RNAs in vascular dysfunction and atherosclerosis. Vascul Pharmacol 2019; 114: 76-92.
9. Zampetaki A, Kiechl S, Drozdov I, et al. Plasma microRNA profiling reveals loss of endothelial miR-126 and other microRNAs in type 2 diabetes. Circ Res 2010; 107: 810-7.
10. Liang Z, Gao KP, Wang YX, et al. RNA sequencing identified specific circulating miRNA biomarkers for early detection of diabetes retinopathy. Am J Physiol Endocrinol Metab 2018; 315: E374-85.
11. Xiong X, Tu S, Wang J, et al. CXXC5: a novel regulator and coordinator of TGF-β, BMP and Wnt signaling. J Cell Mol Med 2019; 23: 740-9.
12. Kim HY, Yang DH, Shin SW, et al. CXXC5 is a transcriptional activator of Flk-1 and mediates bone morphogenic protein-induced endothelial cell differentiation and vessel formation. FASEB J 2014; 28: 615-26.
13. Golledge J. Update on the pathophysiology and medical treatment of peripheral artery disease. Nat Rev Cardiol 2022; 19: 456-74.
14. Ismaeel A, Fletcher E, Miserlis D, et al. Skeletal muscle MiR-210 expression is associated with mitochondrial function in peripheral artery disease patients. Transl Res 2022; 246: 66-77.
15. Barbalata T, Moraru OE, Stancu CS, et al. Increased miR-142 levels in plasma and atherosclerotic plaques from peripheral artery disease patients with post-surgery cardiovascular events. Int J Mol Sci 2020; 21: 9600.
16. Sorrentino TA, Duong P, Bouchareychas L, et al. Circulating exosomes from patients with peripheral artery disease influence vascular cell migration and contain distinct microRNA cargo. JVS Vasc Sci 2020; 1: 28-41.
17. Gallant-Behm CL, Piper J, Dickinson BA, et al. A synthetic microRNA-92a inhibitor (MRG-110) accelerates angiogenesis and wound healing in diabetic and nondiabetic wounds. Wound Repair Regen 2018; 26: 311-23.
18. Kyyaly MA, Sanchez-Elsner T, He P, et al. Circulating miRNAs-A potential tool to identify severe asthma risk? Clin Transl Allergy 2021; 11: e12040.
19. Silva CMS, Barros-Filho MC, Wong DVT, et al. Circulating let-7e-5p, miR-106a-5p, miR-28-3p, and miR-542-5p as a promising microRNA signature for the detection of colorectal cancer. Cancers 2021; 13: 1493.
20. Guo Y, Cui X, Zhang Y, et al. Diagnostic and prognostic value of serum miR-296-5p and miR-28-3p in human gastric cancer. Cancer Biother Radiopharm 2020; 38: 95-101.
21. Liguori M, Nuzziello N, Introna A, et al. Dysregulation of microRNAs and target genes networks in peripheral blood of patients with sporadic amyotrophic lateral sclerosis. Front Mol Neurosci 2018; 11: 288.
22. Wang A, Kwee LC, Grass E, et al. Whole blood sequencing reveals circulating microRNA associations with high-risk traits in non-ST-segment elevation acute coronary syndrome. Atherosclerosis 2017; 261: 19-25.
23. Zhou X, Wen W, Shan X, et al. MiR-28-3p as a potential plasma marker in diagnosis of pulmonary embolism. Thromb Res 2016; 138: 91-5.
24. McDonald AC, Vira M, Walter V, et al. Circulating microRNAs in plasma among men with low-grade and high-grade prostate cancer at prostate biopsy. Prostate 2019; 79: 961-8.
25. Jiménez-Lucena R, Rangel-Zúñiga OA, Alcalá-Díaz JF, et al. Circulating miRNAs as predictive biomarkers of type 2 diabetes mellitus development in coronary heart disease patients from the CORDIOPREV study. Mol Ther Nucleic Acids 2018; 12: 146-57.
26. Zhang J, Yao Y, Li H, et al. miR-28-3p inhibits prostate cancer cell proliferation, migration and invasion, and promotes apoptosis by targeting ARF6. Exp Ther Med 2021; 22: 1205.
27. Skrzypek K, Nieszporek A, Badyra B, et al. Enhancement of myogenic differentiation and inhibition of rhabdomyosarcoma progression by miR-28-3p and miR-193a-5p regulated by SNAIL. Mol Ther Nucleic Acids 2021; 24: 888-904.
28. Lv Y, Yang H, Ma X, et al. Strand-specific miR-28-3p and miR-28-5p have differential effects on nasopharyngeal cancer cells proliferation, apoptosis, migration and invasion. Cancer Cell Int 2019; 19: 187.
29. Zhou X, Feng Y, Liu S, et al. IL-33 promotes the growth of non-small cell lung cancer cells through regulating miR-128-3p/CDIP1 signalling pathway. Cancer Manag Res 2021; 13: 2379-88.
30. Liu YT, Zong D, Jiang XS, et al. miR-32 promotes esophageal squamous cell carcinoma metastasis by targeting CXXC5. J Cell Biochem 2019; 120: 6250-63.
31. Ma L, Wang X, Liu H, et al. CXXC5 mediates P. gingivalis-suppressed cementoblast functions partially via MAPK signaling network. Int J Biol Sci 2019; 15: 1685-95.
32. Yan X, Wu J, Jiang Q, et al. CXXC5 suppresses hepatocellular carcinoma by promoting TGF-β-induced cell cycle arrest and apoptosis. J Mol Cell Biol 2018; 10: 48-59.
33. Chen X, Wang X, Yi L, et al. The KN motif and ankyrin repeat domains 1/CXXC finger protein 5 axis regulates epithelial-mesenchymal transformation, metastasis and apoptosis of gastric cancer via Wnt signaling. Onco Targets Ther 2020; 13: 7343-52.
34. Kühnl A, Valk PJ, Sanders MA, et al. Downregulation of the Wnt inhibitor CXXC5 predicts a better prognosis in acute myeloid leukemia. Blood 2015; 125: 2985-94.
35. Lee SH, Kim MY, Kim HY, et al. The Dishevelled-binding protein CXXC5 negatively regulates cutaneous wound healing. J Exp Med 2015; 212: 1061-80.